Genomic architecture of resistance and tolerance to Swiss needle cast and Rhabdocline needle cast diseases in Douglas-fir

Pooja Singh[1,2,3], J. Bradley St.Clair[4], Brandon M. Lind[5], Richard Cronn[4], Nicholas P. Wilhelmi[6], Mengmeng Lu[1], Dragana Obreht Vidakovic[5], Richard C. Hamelin[5], David C. Shaw[7], Sally Aitken[5], Sam Yeaman[1]

[1] Department of Biological Sciences, University of Calgary, Calgary, AB-T2N 1N4, Canada
[2]Aquatic Ecology Division, Institute of Ecology and Evolution, University of Bern, CH-3012 Bern, Switzerland
[3]Swiss Federal Institute of Aquatic Science and Technology (EAWAG), CH-6047 Kastanienbaum, Switzerland
[4] USDA Forest Service, Pacific Northwest Research Station, 3200 SW Jefferson Way, Corvallis, OR 97331, USA
[5] Centre for Forest Conservation Genetics and Department of Forest and Conservation Sciences, University of British Columbia, Vancouver, BC, Canada
[6] Forest Health Protection, USDA Forest Service, Arizona Zone, Flagstaff, AZ 86001, USA
[7] Department of Forest Engineering, Resources and Management, Oregon State University, Corvallis, Oregon, USA.

Corresponding authors: Pooja Singh (pooja.singh09@gmail.com) and Sam Yeaman (sam.yeaman@ucalgary.ca)

Summary

Understanding the genetic architecture of tolerance and resistance to pathogens is important to monitor and maintain resilient tree populations. Here we investigate the genetic basis of tolerance and resistance and to needle cast disease in Douglas-fir (*Pseudotsuga menziesii*) caused by two fungal pathogens: Swiss needle cast (SNC) caused by *Nothophaeocryptopus gaeumannii*, and Rhabdocline needle cast (RNC) caused by *Rhabdocline pseudotsugae*). We performed a case-control genome-wide association analysis (GWAS) and found these traits to be polygenic. Significant associations with SNC resistance were found for SNPs in genes for stomatal regulation and ethylene and jasmonic acid pathways, which are known for their roles in plant defense and immunity. Top-associated SNPs for SNC tolerance were found in

genes of secondary metabolite pathways. We identified a key upstream transcription factor of plant defence, ERF1, as the main candidate for RNC resistance. Our findings contribute to the understanding of the highly polygenic architectures underlying disease resistance and tolerance in Douglas-fir and have important implications for forestry and conservation as the climate changes.

Key words: GWAS, case-control study, disease resistance, R-genes, fungal pathogens

Introduction

Douglas-fir (*Pseudotsuga menziesii*) is a foundational species in western North America, found in abundance both in coastal rainforests (var. *menziesii*) and in drier, warm continental climates (var. *latifolia*). It is one of the most valuable timber trees and a keystone species in several forest ecosystems. Anthropogenic factors, such as climate change, threaten the health and productivity of Douglas-fir and other forest trees. Pathogens also pose an unprecedented threat to our natural and commercially valuable forests (Smith *et al.*, 2006). Several plant pathogens cause diseases that are known to be exacerbated by climate change, with an increase in epidemics predicted in the future (Bergot *et al.*, 2004; Evans *et al.*, 2008; Juroszek *et al.*, 2020). Identifying genetic variation underlying resistance is crucial to estimate the adaptive potential of plants and develop resistant cultivars. Swiss needle cast (SNC), caused by *Nothophaeocryptopus gaeumannii*, and Rhabdocline needle cast (RNC), caused by *Rhabdocline pseudotsugae*, are two such pathogens causing diseases exclusive to the widespread ecologically and economically important conifer species Douglas-fir (Boyce, 1940; Chastagner, 2001).

SNC is specific to Douglas-fir trees (Boyce, 1940) and the conditions conducive for disease development are primarily present on the coastal subvariety *P. menziesii* var. *menziesii*. This disease is thought to be native to North America but was first described in Switzerland in 1925 and eventually spread across the globe, wherever Douglas-fir is grown (Stone, 2018). The impact of SNC is most severe in the coastal fog zone of British Columbia, Washington, and Oregon (Figure 1A) and has worsened over the last 40 years (Hansen *et al.*, 2000; Black

et al., 2010; Shaw *et al.*, 2021). *Nothophaeocryptopus gaeumannii* spores germinate under conducive conditions of humidity and temperature in late spring and early summer. The hyphae enter young Douglas-fir needles via the stomata and the fungus occupies the intercellular spaces (Capitano, 1999) (Figure 1B). The reproductive structures (pseudothecia) of *N. gaeumannii* block the stomata, interfering with gas and water exchange (Manter *et al.*, 2001; Swiss Needle Cast Collective, 2011). Needle CO_2 uptake decreases as the pseudothecia increase in density. Once 25% of the stomata are occluded, net CO_2 uptake is zero, and foliage retention decreases (Manter *et al.*, 2000, 2003). The symptoms of SNC are foliage chlorosis and premature needle abscission 1–4 years following infection (Ritóková *et al.*, 2016). This inevitably results in reduction in tree growth, but tree mortality as a result is rare (Shaw *et al.*, 2011). As much as 50% growth loss has been reported in coastal Oregon populations since 1990 from SNC epidemics (Maguire *et al.*, 2002), presenting a substantial forest health problem (Shaw *et al.*, 2021). Though it must be noted that unlike other fungal pathogens, *N. gaeumannii* is an endophyte that relies on living host cells and is not expected to induce a strong immune response. However, the occlusion of the stomata during SNC infection is concerning because Douglas-fir trees, and conifers in general, represent a major terrestrial carbon sink. (Stone *et al.*, 2008a) show that hyphae of *N. gaeumannii* oppress against cells of the palisade parenchyma and spongy mesophyll and may form mucilage where they contact the cell. It could be that the fungus is influencing membrane permeability and getting nutrients from the cell without direct penetration by hyphae. This could indicate a more direct interaction of *N. gaeumannii* with the leaf than being merely a passive endophyte. However, evidence of *N. gaeumannii* triggering an immune response is lacking.

Local climate likely plays a role in the pathogenicity of *N. gaeumannii* because the most severe symptoms are found in the low-elevation coastal fog zone and infections have increased in severity in these zones since 1980 (Black *et al.*, 2010). Subsequent disease prediction models have found that warmer winter temperatures and greater spring and summer precipitation in previous years strongly correlates with SNC abundance and severity in the following years (Stone *et al.*, 2008b; Wilhelmi *et al.*, 2017). With climate change resulting in warmer temperatures, the zone in which *N. gaeumannii* severity is high is projected to expand to higher elevations and inland in Oregon (Lee *et al.*, 2017) and on the BC Coast, and become a major environmental challenge beyond the coastal fog belt.

Douglas-fir is host to another foliar fungal pathogen, *Rhabdocline pseudotsugae,* which causes RNC in the coastal Pacific Northwest United States and Canada (British Columbia) (Chastagner, 2001); Figure 1C, D) and has since spread to Europe.

The infection of *R. pseudotsugae* is thought to be associated with local environments, particularly moisture (Wilhelmi *et al.*, 2017, 2021). Similar to *N.gaeumannii,* ascospores of Rhabdocline spp. are released in late spring/early summer, coinciding with bud burst and shoot elongation of Douglas-fir. Rhabdocline spp. require similar environmental conditions as N.gaeumanni with high humidity, rain, and mild temperatures most conducive to spore release and infection (Parker, 1970; Chastagner, 1990). Infections are initiated by the germination of mature ascospores on the needle surface. Contrary to *N. gaeumannii*, infection takes place directly through the cuticle of the needle (Brandt, 1960), and the fungus then grows within the needle. Also contrary to *N. gaeumannii*, an infection by *Rhabdocline* spp. kill host cells as it progresses through the needle. This process produces mottled chlorosis and necrotic spots which become noticeable in the late summer/early fall. Colonisation of the needle continues through the winter, and necrotic spots and mottled chlorosis begin to coalesce giving the foliage a characteristic chlorotic yellow to light brown color. In early spring, apothecia (fruiting structures of Rhabdocline spp.) emerge from below the epidermis. The fruiting bodies eventually rupture through the epidermis exposing the asci and releasing ascocpores to infect newly emerging Douglas-fir foliage. Needles are generally cast in the early summer, shortly before or after fruiting bodies emerge (Brandt, 1960; Chastagner, 1990; Wilhelmi *et al.*, 2021). Decreases in growth due to the loss of foliage related to Rhabdocline infection are estimated to be as high as 50% for trees with moderate to severe infection (Kurkela, 1981).

A tractable approach to improve tree health and resilience to pathogens is to understand and deploy the innate tolerance and resistance mechanisms of trees. Plant resistance mechanisms reduce the probability of pathogen infection and tolerance mechanisms reduce loss of fitness even when infected (Restif & Koella, 2004). For this study we will hereon refer to ‘resistance’ as the tree defence responses that reduce pathogen abundance and ‘tolerance’ as the tree’s ability to continue to grow and retain its leaves, even in the presence of the

pathogen *sensu* Wilhelmi *et al*. (2017). In coastal Douglas-fir populations where SNC infections can be severe, trees have evolved resistance and tolerance to SNC (Shaw *et al.*, 2011; Lee *et al.*, 2017). This is not the case for interior Douglas-fir (*Pseudotsuga menziesii* var. *glauca*) where disease incidence is much lower. Wilhelmi *et al*. (2017) found evidence for genetic variation across populations in the Pacific North-West for SNC tolerance (but not resistance) and RNC resistance. This local adaptation for SNC tolerance and RNC resistance is consistent with how plant pathosystems evolve (Wilhelmi *et al.*, 2017). In addition to among population variation, there is within population genetic variation for SNC tolerance in Coastal Douglas-fir (Johnson, 2002). The difference in tolerance/resistance between SNC and RNC is attributed to their different infection modes: *R. pseudotsugae* is a necrotroph that kills host cells to feed while *N. gaeumannii* is a biotroph that is endophytic and its nutrition depends on living host cells (Brandt, 1960; Capitano, 1999). Even though SNC epidemiology and *N. gaeumannii* pathogenicity are well studied, the molecular genetic basis of resistance/tolerance to this disease is poorly understood. RNC epidemiology is well known, and there is some genetic basis in resistance (Wilhelmi *et al.*, 2017, 2021; Stone, 2018).

Genome-wide association studies (GWAS) have played a crucial role in identifying genomic regions associated with pathogen resistance in wild and domesticated plants (Zhu *et al.*, 2008). Here we employ a GWAS approach to understand the genomic basis of tolerance and resistance to needle cast fungal diseases in Douglas-fir trees from North-Western USA. Our statistical analysis has been adapted for Douglas-fir exome pooled-sequencing data from multiple populations with 20 or fewer individuals per population. A case-control design compares marker frequencies between a group of disease resistant (or tolerant) individuals (cases) and a group of disease intolerant individuals (controls). Our aim was to examine the genomic architecture of disease tolerance and resistance in Douglas-fir and identify candidate genes associated to SNC and RNC. The resistant and tolerant SNPs from our study have been included in a SNP array for use in genomic selection in forestry management and conservation of Douglas-fir (Lind, Lu *et al.* in prep).

Materials and Methods

Sampling, study design, and disease phenotyping

A Seed Source Movement Trial (SSMT) was used to evaluate resistance and tolerance to SNC and resistance to RNC in 60 Douglas-fir populations from 12 geographic regions in Oregon, Washington and California (see Wilhelmi et al 2017 for details, File S1, Figure S1). Each region was represented by five populations and each population was represented by open-pollinated seed from two parent trees naturally regenerated within a stand (File S1). Parents were located 100m apart to avoid inbreeding. The seed source and test sites were used to capture the climatic gradients experienced by *P. menziesii* var. *menziesii*. Adult trees in the common gardens were surveyed for overall tree health ranging from 0 to 3 based on crown density, crown colour and needle retention. SNC-resistant individuals were identified as those with overall health of 0 or 1. Of the remaining individuals with overall health index >1, infection status for SNC was assessed based on an index combining the following phenotype criteria: (A) Crown density was rated on a scale ranging from 1-4, with a 1 corresponding to a sickly sparse crown lacking in needle retention and a 4 corresponding to a full healthy crown; (B) Crown colour was rated on a scale from 1-3, with a 3 corresponding to a green healthy crown color and a 1 corresponding to highly chlorotic, sickly crown colour; (C) Needle retention was rated on a secondary lateral branch located on the fourth whorl and on the south side of the tree, and was estimated as the proportion of needles retained in each year of growth (e.g., 1.5 refers to a tree holding 100% of its current year needles, 50% of its second-year needles and no third-year needles). As crown density was considered the most representative measure, an index of overall severity of infection was calculated as the sum of 2A + B + C. Pools of tolerant and intolerant individuals were constructed within each site*region combination by picking the highest- and lowest-ranked individuals from each family using this index. The final dataset for SNC contained 13 Resistant (R) pools, 55 Tolerant (T) pools and 55 Intolerant (I) pools. For RNC, severity was assessed as a single index from 0 (least severe) to three (most severe). Pooling for RNC was conducted as above, but there were many fewer populations infected, so for RNC we had 5 Resistant (R) and 5 Intolerant (I) pools.

Probe design and sequencing

We used a pool-sequencing approach that targeted exon regions. For probe design details see (Lind *et al.*, 2022). Briefly, the sequence capture probes were designed using genes identified in Douglas-fir RNA-seq data from (1) daily and cyclic induced experiments (Cronn *et al.*, 2017) and (2) needles samples infected by the fungal pathogen causing SNC *Nothophaeocryptopus gaeumannii* and wasp (unpublished). Exon sequences with a length of at least 100bp were submitted to Roche NimbleGen for Custom SeqCap EZ probe design.

DNA was extracted from Douglas-fir diploid needle tissue. DNA samples were normalised at 10ng/µl and 10 to 20 individuals were pooled per site (See File S2) by combining equimolar amounts of individual DNA samples prior to library preparation. Barcoded (Kapa, Dual-Indexed Adapter Kit) libraries were made using 100-150ng of DNA from each pooled DNA sample with an approximately 450-bp mean insert size. SeqCap library preparation was performed using custom Nimblegen SeqCap probes according to the NimbleGen SeqCap EZ HyperCap Workflow User's Guide Ver 2 (Roche Sequencing Solutions, Inc., CA USA). Following capture, each library was sequenced in a 150bp paired-end format on an Illumina NovaSeq 6000 instrument at the Genome Quebec Innovation Centre (McGill University, Montreal, Canada).

Mapping and SNP calling

As in (Lind *et al.*, 2022), we used the VarScan pipeline (Lind, 2021a) to process our genomic data. Raw sequence reads were trimmed with fastp (v0.19.5, Chen et al. 2018) by trimming reads that did not pass quality filters of less than twenty N's, a minimum mean Phred quality score of 30 for sliding windows of five base pairs, and a final length of 75 base pairs with no more than 20 base pairs called as N (-n 20 -M 30 -W 5 -l 75 -g -3). Trimmed reads were mapped with bwa-mem (v0.7.17, Li & Durbin 2009) to the congeneric Douglas-fir *Pseudotsuga menziesii var. menziesii* reference (v1.0) (Wegrzyn *et al.*, 2014). This reference was extended by including non-redundant contigs from an in-house Douglas-fir SNC infected needle transcriptome assembly. The mapped read .sam files were converted to binary with SAMtools v1.9 (view, sort, index; Li et al. 2009) and subsequently filtered for proper pairs and a mapping

quality score of 20 or greater (view -q 20 -f 0x0002 -F 0x0004). Using Picard tools v2.18.9 (http://picard.sourceforge.net), read groups were added and duplicates subsequently removed from filtered bam files. Indel realignment was performed with GATK 3.8 (McKenna et al. 2010). SNP calling was done using VarScan (v2.4.3; Koboldt et al. 2012) by passing a SAMtools mpileup object directly to VarScan::mpileup2cns with a minimum coverage set to 8, -value < 0.05, minimum variant frequency of 0.00, ignoring variants with >90% support on one strand, a minimum average genotype quality of 20, and a minimum allele frequency of 0.80 to call a site homozygous (--min-coverage 8 --p-value 0.05 --min-var-freq 0.00 --strand-filter 1 --min-avg-qual 20 --min-freq-for-hom 0.80). Global allele frequency was calculated by multiplying each pool's ploidy (2N) by the pool's ALT allele frequency, summing these products, and dividing by the total ploidy across populations. The output was filtered with a custom python (v3.7, www.python.org) script to remove indels, keeping only biallelic loci, genotype quality score > 20, and filter for global minor allele frequency ≥ 0.05. SNP contingency tables were generated by calculating REF/ALT allele counts by multiplying the total ploidy of the pool (2 * number of individuals) by the ALT allele frequency or 1- ALT allele frequency. SNPs flagged as being paralogs by (Lind *et al.*, 2022) were discarded. Code for the SNP calling pipeline can be found here: https://GitHub.com/CoAdapTree/varscan_pipeline.

Cochrane-Mantel-Haenszel (CMH) test

A case-control method was implemented to identify loci associated with SNC and RNC tolerances/resistance. Using output from the VarScan pipeline (Lind, 2021a) we performed GWAS using a modified Cochrane-Mantel-Haenzel (CMH) test implemented in python (Lind, 2021b) across stratified contingency tables. Here, each stratum pertains to a single population, where each population has a 'case' and a 'control' pool. Each contingency table is 2x2 - case and control x REF and ALT allele counts. ALT and REF allele counts are calculated by multiplying the ploidy of the pool (2N) by either the ALTfreq or (1 - ALTfreq), respectively. This step converts read depth into pseudo-counts, which represent our real replication level. Pseudo-counts are necessary because sequencing coverage per pool exceeds the number of individuals in each pool, resulting in resampling of same allele from a single individual several times. Our tested case-control comparisons for SNC were as follows (1) Intolerant versus Tolerant, (2) Tolerant versus Resistant, and (3) Intolerant versus Resistant

comparisons. For RNC, susceptible versus resistant groups were contrasted to identify SNPs associated with resistance. Code for the CMH pipeline is available here: https://github.com/CoAdapTree/cmh_test. False discovery rate (FDR) correction was applied with a threshold of <0.05 for significance. Finally, we tested for enrichment in outlier status between groups of SNPs identified among the three SNC case-control comparisons using the hypergeometric test in R v4.0.5.

Extended annotation and Gene Ontology enrichment

The existing Douglas-fir genome annotation (v1.0) from treegenesdb.org (Neale *et al.*, 2017) was improved for this study by including genes expressed in Douglas-fir needles during (1) SNC infection (2) wasp infection and (3) cyclic rhythms. The SNC and wasp mRNA-seq data were generated for this study and the cyclic mRNA-seq data were from (Cronn *et al.*, 2017). The RNA-seq reads were assembled *de novo* using Trinity (v2.8.5, (Grabherr *et al.*, 2011) into 83,829 transcripts with 42,616 cyclic-induced transcripts; 26,261 wasp-induced transcripts; and 14,952 SNC-induced transcripts. The assembled transcripts were mapped to the Douglas-fir reference genome using GMAP (v2019-03-15) and any previously unannotated genes were appended to the existing annotation, producing a Douglas-fir merged annotation with 94,716 genes. The high number of annotated genes are a result of merging gene annotations from different tissues and assembly sources. Overlap of genes between case-control groups was tested using the hypergeometric test in R v4.0.5. Functional annotation of the assembled transcriptome was conducted using EnTAP (Hart *et al.*, 2020). Gene Ontology (GO) enrichment of Biological Process (BP), Molecular Function (MF) and Cellular Component (CC) was conducted using EnTAP annotation topGO (v2.38.1) (Alexa & Rahnenfuhrer, 2019).

Linkage Disequilibrium (LD) decay estimation

To estimate a proxy related to species-wide linkage disequilibrium (LD), we calculated the correlation in allele frequency among SNPs across all populations using squared Spearman's rank correlation coefficient, ρ^2 (Hill & Robertson, 1968). To calculate background LD, we randomly selected 10,000 SNPs across the genome, then identified all the contigs harbouring

those 10,000 SNPs and then calculated r^2 among all pairwise combinations of SNPs within each contig. This resulted in us calculating background r^2 within each of 19,095 contigs. The non-linear decay of r^2 with genomic distance was fitted using Hill and Weir expectation of r^2 between neighbouring sites (Hill & Weir, 1988), which is derived for a single population but should give an approximately accurate shape for the expected rate of decay of r^2 with physical distances. We used the equation:

$$E(r^2) = [10+C(2+C)(11+C)] * [1+ n(3+C)(12+12C+C^2)(2+C)(11+C)]$$

where n is sample size, C is the product of the population recombination parameter ($\rho = 4N_e r$) and the distance between SNPs in base pairs as implemented in (Remington *et al.*, 2001; Marroni *et al.*, 2011). Nonlinear least squares were used to fit this equation to SNC data using the R package *nls*. LD decay or LD half-life was calculated as the point when the observed r^2 between sites decays to less than half the maximum r^2 value. To evaluate the extent of LD around GWAS significant SNPs, we calculated r^2 for all SNPs (neutral and significant) on contigs that contained at least one significant GWAS SNP (for each pool). Using the fitted background LD, we calculated residual LD for all contrasts with the GWAS significant SNPs.

Results

GWAS analysis of Douglas-fir response to Swiss Needle Cast (SNC)

77 - 85% reads across pools mapped to the reference Douglas-fir genome. 672,965 SNPs were retained after filtering across 13 Resistant (R) pools, 55 Tolerant (T) pools and 55 Intolerant (I) pools (Figure S2A). We identified 1320 significant SNPs (*p.adjust* < 0.05 FDR corrected) for $SNC_{I\ vs\ R}$ case-control comparison; 1095 significant SNPs (*p.adjust* < 0.05 FDR corrected) for $SNC_{T\ vs\ R}$ case-control comparison; and 182 significant SNPs (*p.adjust* < 0.05 FDR corrected) for $SNC_{I\ vs\ T}$ case-control comparison (Figure 1E, File S3). The $SNC_{I\ vs\ R}$ and $SNC_{T\ vs\ R}$ had a significant overlap of 84 SNPs (expected overlap = 2.1; p < 1e-15), thus we identified 2,330 (1320+1095-85) SNC resistance-associated SNPs. The $SNC_{I\ vs\ R}$ and $SNC_{I\ vs\ T}$ had a significant overlap of 3 SNPs SNPs (expected overlap = 0.4; p = 5.7e-3; Figure 1E). The $SNC_{I\ vs\ T}$ and $SNC_{T\ vs\ R}$ analysis had no overlap in SNPs.

We annotated significant GWAS SNPs with the Douglas-fir genome annotation (treegenesdb.org). $SNC_{I\ vs\ R}$ SNPs mapped to 614 genes, $SNC_{T\ vs\ R}$ SNPs mapped to 541 genes, and $SNC_{I\ vs\ T}$ SNPs mapped to 82 genes (Figure 2A, File S3). There were no genes overlapping among all three comparisons. 76 genes significantly overlapped between the $SNC_{I\ vs\ R}$ and the $SNC_{T\ vs\ R}$ comparisons (p < 1e-15; expected overlap = 10; Figure 2A, File S3). Four genes significantly overlapped between the $SNC_{I\ vs\ R}$ and $SNC_{I\ vs\ T}$ comparisons (p = 0.02; expected overlap = 1.6) and two genes overlapped between the $SNC_{T\ vs\ R}$ and $SNC_{I\ vs\ T}$ comparisons (not significant p = 0.14; expected overlap = 1.3) (Figure 2A, File S3). Overall, we found 1073 unique candidate genes underlying resistance to SNC, 76 unique candidate genes underlying tolerance to SNC, and six candidate genes potentially involved in both resistance and tolerance to SNC.

Most candidate genes had one significant SNP per gene, but some genes had up to 16 significant SNPs (Figure 2B). The genes with the highest number of significant SNPs were identified from the $SNC_{I\ vs\ R}$ and $SNC_{T\ vs\ R}$ analyses and thus are putatively involved in SNC resistance. Candidate genes for SNC tolerance from the $SNC_{I\ vs\ T}$ analysis had a maximum of three SNPs per gene. Notably, the gene TPR1 (topless-related protein 1) had 16 significant SNPs; CYP78A4 (Cytochrome P450 78A4) had 9 significant SNPs; cyclic_GAZW02100664.1 (gene expressed in circadian rhythm) and GTG2 (GPCR-type G protein 2) had eight significant SNPs each; three transcripts wasp (MSTRG.42441.3_MSTRG.42441, wasp_MSTRG.42442.1_MSTRG.42442, snc_MSTRG.7080.1_MSTRG.7080) expressed in wasp and SNC induced libraries had seven significant SNPs each; and RNF8A (E3 ubiquitin-protein ligase rnf8-A), PRR (pentatricopeptide repeat-containing protein) and DCR (BAHD acyltransferase DCR-like) has six significant GWAS SNPs each (File S3).

Gene Ontology (GO) enrichment of SNC candidate genes

We tested GO enrichment of biological processes for the top 100 genes (ranked based on p-values from the GWAS analysis) for each of three SNC case-control comparisons (File S3). Relevant enriched GO terms for $SNC_{I\ vs\ R}$ were immune system process, regulation of defense

response, jasmonic acid biosynthetic process, response to biotic stimulus, response to chitin and response to wounding (File S4). Relevant enriched GO terms for $SNC_{T\ vs\ R}$ were immune system process, negative regulation of the ethylene signalling pathway, and stomatal closure and movement (File S4). Relevant enriched GO terms for $SNC_{I\ vs\ T}$ were immune system process, flavonoid, phenol, terpenoid, lignin, and antibiotic metabolic processes (File S4). Candidate genes annotated with defense or immune response functions were: TPR1, GTG2, HIR1, OPR2, RD19B, PAD4 and CYP78A4 from the $SNC_{I\ vs\ R}$ comparison; ETR2, LOX, PER21, PRR and SDH from the $SNC_{T\ vs\ R}$ comparison; and FMO1, RD19B and At5g63020 (a predicted R gene) from the $SNC_{I\ vs\ T}$ comparison (File S3).

Linkage disequilibrium (LD) of significant SNC SNPs

We defined LD decay as the point when the observed r^2 between SNPs decays to less than half the maximum r^2 value. The background LD decay distance across the genome calculated using all SNPs across a random subset of 19,095 contigs was 224 bp (Figure 3A, Figure S3). Compared to the background, the LD decay distance of $SNC_{I\ vs\ R}$ SNPs was the largest at 1260 bp, followed by $SNC_{T\ vs\ R}$ SNPs at 762 bp, and the $SNC_{I\ vs\ T}$ SNPs at 450 bp (Figure 3A, Figure S3). Thus, SNC resistance-associated SNPs exhibited higher LD than SNC tolerance-associated SNPs, which is suggestive of stronger selection on the SNC resistance-associated SNPs. Natural selection on both SNC tolerant and resistance-associated SNPs would be expected to result in genetic hitchhiking of neutral alleles on the same contig. To look for this signature, we also analysed the relationship between the number of significant SNC associated SNPs found per gene and pattern of LD across that gene (Figures 3B-D). To represent the amount of LD across a gene relative to the background expectation, for each pairwise combination of SNPs we represented their observed LD as a residual relative to the LD decay model that was fit to the background SNPs and took the average across these residuals. As expected, due to genetic hitchhiking hypothesis, we found a significant positive relationship between the number of SNPs associated with SNC resistance in a gene and the average residual-LD across those genes for candidate genes from the SNC T vs R comparison (pvalue = 0.005, correlation = 0.12, Figure 3D). This relationship was not significant for genes from the SNC IvsR comparison or the SNC IvsT comparison (Figure 3B, C).

GWAS analysis of Douglas-fir response to Rhabdocline Needle Cast (RNC)

80-84 % reads from RNC pools mapped to the reference Douglas-fir genome. 1,016,287 SNPs were retained after filtering across 5 Intolerant (I) and 5 Resistant (R) pools (Figure S2B). We identified four significant SNPs (*p.adjust* < 0.05) for $RNC_{I\ vs\ R}$ case-control comparison (Figure 1E, File S3). The RNC significant SNPs had no overlap with SNC significant SNPs. We estimated the correlation of the allele frequencies of the four SNPs in our dataset as a proxy for LD and found three SNP are in a cluster of high LD with each other (Spearman's $\rho > 0.6$; Figure 4A). We annotated the four RNC significant SNPs and only one mapped to two genes (not fully overlapping) located on opposite strands, while the other three SNPs were intergenic. On the - strand was Eukaryotic Release Factor 1 (ERF1) and on the + strand was the Eurkaryotic Release Factor 105 (ERF105) (File S3).

Discussion

The eco-evolutionary dynamic of climate change and plant pathogens has increased the severity of disease in agricultural and wild plant communities (Garrett *et al.*, 2006). However, our limited understanding of the genetic, adaptive, and mechanistic patterns of plant-pathogen interactions impedes critical management and conservation decisions. This makes empirical studies delineating the genetic basis of disease resistance crucial. Here we investigated the genetic basis of resistance of two needle-cast disease-causing fungi in economically and ecologically important Douglas-fir using a case-control approach to genome-wide association analyses. We found SNC resistance and SNC tolerance in Douglas-fir to have polygenic and largely non-overlapping genomic architectures. Our analyses identified a suite of candidate genes for SNC tolerance/resistance and RNC resistance involved in key plant immunity pathways and shed light on the signatures of selection in these genes.

Tolerance and resistance represent two major plant defence mechanisms (Baucom & De Roode, 2011). While pathogen resistance has been extensively studied, tolerance is less understood in comparison because disease resistance is considered evolutionarily more important (Pagán & García-Arenal, 2018). In contrast, it has been hypothesised that tolerance

and not resistance is the primary defense mechanism of Douglas-fir trees against SNC because *N. gaeumannii* is an endophyte (Temel *et al.*, 2004, 2005). However, neither the genetic basis of tolerance nor resistance to SNC is well understood, even though this disease has had a major impact on the forestry economy of the Pacific Northwest and its severity increasing with climate change is increasing this impact (Shaw *et al.*, 2021). We found that both resistance and tolerance to SNC had complex genetic architectures involving hundreds of SNPs, which may reflect the complex pathology of this disease (Stone, 2018; Montwé *et al.*, 2021). Plant disease resistance is a highly quantitative trait (Young, 2003), therefore our discovery of more than one thousand candidate genes associated with SNC resistance is not surprising. However, contrary to previous studies that suggest that disease tolerance involves few genes (Pagán & García-Arenal, 2018), we identified many candidate genes associated with SNC tolerance. This suggests that tolerance to SNC in Douglas-fir, and tolerance perhaps more broadly in plants, may be much more complex genetically than previously thought, where selection can target multiple points in (perhaps multiple) physiological pathways that can lead to pathogenic tolerance.

Disease tolerance and resistance mechanisms in plants are known to coexist and evolve simultaneously(Restif & Koella, 2004). While most plant defence evolutionary models assume the two mechanisms to be independent, it has been shown that they can be co-dependent too (Howick & Lazzaro, 2017). We found small overlap of only three SNC resistant and tolerance-associated SNPs, which suggests that the genetic bases of tolerance and resistance to SNC in Douglas-fir are distinct. This was also echoed in only six candidate genes being associated with both SNC resistance and tolerance. The non-overlapping genomic architectures of these two SNC defence mechanisms in Douglas-fir may allow them to evolve independently and reduce constrains imposed by genetic trade-offs (Howick & Lazzaro, 2017). One of the six overlapping genes was the cysteine protease RD19B that is known to play a role in pathogen resistance in *Arabidopsis thaliana* (Bernoux *et al.*, 2008). Given that each of these pairs of contrasts involves repeated use of the same pool of individuals (e.g. both I vs. R and T vs. R involve comparison with the R strain), this limited overlap is particularly noteworthy as more overlap might be expected given the nonindependence of the comparisons.

Plants have evolved constitutive and induced immunity for defense against pests and pathogens (Freeman & Beattie, 2008). Constitutive defenses consist of structural barriers that

prevent infection such as waxy cuticles and cell wall. Induced defenses involved the production of chemicals, enzymes that degrade pathogen cells or cause programmed host cell death (Freeman & Beattie, 2008). There are two categories of induced resistance (1) Systemic acquired resistance (SAR), which is a salicylic acid dependent process that produces pathogenesis related (PR) proteins (Lefevere *et al.*, 2020); (2) Induced systemic resistance (ISR), which is mediated by the phytohormones ethylene and jasmonate and does not involve PR proteins (Hammerschmidt, 1999). We found the gene COMT, which is involved in lignin biosynthesis, to be associated with SNC resistance and this provides a clue that lignin biosynthesis might be involved in resistance to *N. gaeumannii* (Ma & Xu, 2008). Lignin is another secondary metabolite found in fir needles and lignin deposition can also act as a physical barrier restricting pathogen growth as lignin is a polymer that is very recalcitrant to degradation (Lee *et al.*, 2019). Furthermore, we found that genes associated with SNC resistance were enriched with GO terms related to defense response as well as the jasmonic acid and ethylene signalling pathways, which play a key role in plant immunity (Miller *et al.*, 2017). Interestingly, regulation of stomatal closure and movement were also enriched GO terms for SNC resistance genes. This may point to stomatal regulation during *N. gaeumannii* infection as an important defense response. Swiss Needle Cast-resistance genes were also involved in responses to biotic stress and chitin. This could reflect the interaction of cells in the needles of Douglas-fir with *N. gaeumannii*, as fungal cell walls contain chitin and plant cell walls do not (Pusztahelyi, 2018). Plants have evolved immune responses that detect fungal chitin as a microbe-associated molecular pattern (Pusztahelyi, 2018). The 'response to wounding' GO term that was enriched in SNC resistance genes may refer to the abscission of needles caused by SNC or reflect a general response to infection. Interestingly, SNC tolerance genes were enriched for flavonoid, phenol, terpenoid, lignin metabolic process and antibiotic metabolic process. Flavanoids, phenols, and terpenes are secondary metabolites that can function as antibiotics in plants (Falcone Ferreyra *et al.*, 2012; Sharma *et al.*, 2017; Tuladhar *et al.*, 2021). Overall, we find that plant phytohormones play a larger role in SNC resistance and secondary metabolites play a larger role in SNC tolerance in Douglas-fir. Plants produce phytohormones to rapidly and specifically respond to environmental stressors, such as fungal pathogens.

One of the most intriguing candidate genes for SNC resistance was the AS1-like gene, which is a transcription factor that negatively regulates inducible resistance against pathogens by

binding to promoters of the jasmonic acid pathway (Nurmberg *et al.*, 2007). Loss of function mutations of AS1 were found to increase resistance against necrotrophic fungi in *A. thaliana* and thus function was evolutionarily conserved in plants spanning a 125 Ma of divergence time (Nurmberg *et al.*, 2007). Another important candidate gene for SNC resistance was GTG2, a G-protein coupled receptor for abscisic acid (Pandey *et al.*, 2009). G-proteins are known to play a role in plant immunity by regulating stomatal closure, restricting pathogen invasion (Zhang *et al.*, 2012). Abscisic acid is one of the best studied regulators of stomatal closure (Wang *et al.*, 2011). Pattern-recognition receptor (PRR) was another key candidate gene found in our study. PRRs are important plant receptors that activate immune response after detecting pathogen associated molecular patterns (Wang & Chai, 2020). Other important candidates for SNC resistance were PAD4, which plays a role in salicylic acid-dependent plant defense against pathogens (Jirage *et al.*, 1999); LOX gene, known to play a role in plant defense by programmed cell death hypersensitive response at the site of necrosis (Rustérucci *et al.*, 1999; Kolomiets *et al.*, 2000); PER21, a member of peroxidase family that are evolutionarily conserved and involved in plant defense responses against pathogenic fungi (Mir *et al.*, 2015); SDH, a succinate dehydrogenase that regulates plant defense to fungi in potatoes via the salicyclic acid pathway (Zhang *et al.*, 2020); a DCR-like gene that plays a key role in the formation of cutin, which is a key component of the plant cuticle that acts as a physical defense barrier against invading fungal pathogens (Panikashvili *et al.*, 2009; Serrano *et al.*, 2014); a probable Resistance (R) gene: the LRR receptor-like serine/threonine-protein kinase (At1g67720); and the FMO1 gene, a flavin dependent monooxygenase that is a crucial component of acquired systemic resistance against pathogens (Mishina & Zeier, 2006). All this evidence points to a strong immune response from Douglas-fir to *N. gaeumannii* infection. This contradicts previous thinking about the endophytic nature of *N. gaeumannii* compared to necrophytic fungal pathogens prevents it from triggering host immunity.

Pathogens impose selection pressure on their hosts. Positive selection occurs when an allele favored by natural selection increases in frequency in the population. Due to genetic hitchhiking, neighboring linked neutral alleles also increase in frequency, reducing nearby variation, which results in selective sweeps (Maynard Smith & Haigh, 1974; Barton, 2000). Such signatures of positive selection can be detected by searching for regions of reduced variation or elevated LD patterns introduced by selective sweeps across the genome (Nielsen, 2005). While we lost haplotype information with our pool-seq datasets, we use the correlation of allele frequencies across populations between loci as a proxy for LD. This method was

highly correlated to haplotype-derived estimates (Lucek & Willi, 2021). We found that the LD decay on contigs with SNC resistance-associated SNPs was 5-fold higher than from random background contigs, and LD decay on contigs with SNC tolerance-associated SNPs was 2-fold higher than random background contigs. This LD patterns suggest that SNC tolerance and resistance-associated SNPs are experiencing positive selection in Douglas-fir and that selection is stronger on resistance-associated SNPs than the tolerant SNPs.

Another indicator of the strength of selection is the number of significantly associated SNPs (Figure 2B). Candidate genes for SNC resistance phenotypes had some of the highest number of significant SNPs per gene, suggesting that they are under stronger selection than SNC tolerance genes (Figure 3). However, the large number of significant SNPs does not directly indicate many selected causal SNPs, it could also arise indirectly due to selection, causing flanking SNPs to have similar allele frequency patterns (Mitchell-Olds *et al.*, 2007). We found a positive relationship between number of significant SNPs per genes and the landscape of LD around that gene, suggesting that selection on causal SNC resistance-associated variants was causing an elevation in LD. As this relationship did not hold for SNC tolerance-associated SNPs, we conclude that selection is stronger on SNC resistance in Douglas-fir than SNC tolerance and that the number of causal variants underlying SNC resistance is much lower than identified here. Of the candidate SNC resistance genes that had many SNPs, of note was the gene TPR1 that contains 16 significant SNPs. This gene has been shown to activate TIR-NB-LRR R protein-mediated immune responses by repressing its negative regulators in *A. thaliana* (Zhu *et al.*, 2010). The GTG2, PRR, and DCR-like genes discussed above had six or more outlier SNPs each. While likely driven in part by hitchhiking with strong selection, this high number of significant SNPs in SNC resistance genes may also represent selection on multiple causal variants, as the result of the plant-pathogen arms race that requires plant R genes to constantly evolve to keep up with the evolutionary trajectory of the pathogen (Yang *et al.*, 2013).

The most strongly associated candidate gene for RNC resistance was ERF1, a member of the ERF/AP2 transcription factor family. ERF1 acts downstream of two major plant immunity pathways (ethylene and jasmonate signalling, Figure 4B), regulating pathogen response genes that inhibit disease progression (Lorenzo *et al.*, 2003). It is possible (but unlikely) that RNC resistance in Douglas-fir involves only one large effect gene. However, it is more likely that

our statistical power to detect more RNC resistance-associated SNPs was limited by the few individuals that were sampled for this GWAS comparison. There was no overlap in the candidate SNPs or genes for SNC and RNC, this was partly expected as the two fungal pathogens have very different pathological behaviours (Stone *et al.*, 2008b,a). However, there is an overlap in the plant immunity pathways, ethylene and jasmonate, that are involved in both RNC and SNC resistance. Interestingly, the ERF1 is locally adapted to summer heat moisture and Hargreaves climate moisture deficit environmental variables in natural populations of coastal Douglas-fir (Lind et al, Baypass results, in prep). This is striking as *R. pseudotsugae* spore release is dependent on moisture available through high humidity, dew or rainfall (Wilhelmi *et al.*, 2021). It also implies that climate change will impact the ability of Douglas-fir trees to response to RNC.

In conclusion, our study sheds light on the polygenic genomic architectures of tolerance and resistance to the little understood needle cast diseases SNC and RNC in Douglas-fir. The SNP-array that we designed using the SNPs from this study pave the way for improved genomic selection in forestry management and conservation of Douglas-fir trees.

Acknowledgements

We would like to acknowledge the traditional territories of the peoples of the Treaty 7 region in Southern Alberta and the traditional, ancestral, unceded territory of the Musqueam First Nation where this research was conducted. The CoAdapTree project is funded by Genome Canada (241REF; Co-Project Leaders SNA, SY and Richard Hamelin), with co-funding from Genome BC and 16 other sponsors (http://coadaptree. forestry.ubc.ca/sponsors/), including Genome Alberta, Génome Québec, the BC Ministry of Forests, Natural Resources Operations and Rural Development, Alberta Innovates Bio Solutions, Vernon Seed Orchard Company, University of Alberta, University of British Columbia, Compute Canada, Mosaic Forest Management, and Western Forest Products. We would also like acknowledge funding from NSERC Discovery (SY, SA), Alberta Innovates, Compute Canada; and the United States Forestry Service. We thank Centre d'expertise et de services Génome Québec for sequencing service.

Author contributions

Pooja Singh: Conducted main bioinformatic analyses, Wrote the manuscript
L. Bradley StClair: Conceived study, established study design, sampling, phenotyping
Brandon M. Lind: SNP calling, CMH test pipeline, GO annotations of Douglas fir genes
Richard Cronn: Sampling, DNA extraction
Nicholas P. Wilhelmi: Sampling, phenotyping
Mengmeng Lu: Designed the poolseq probes, modified CMH test
Dragana Obreht Vidakovic: Library construction
Richard Hamelin: Conceived study, acquired funding
Sally Aitken: Conceived study, acquired funding
Dave Shaw: Sampling and phenotyping design
Sam Yeaman: Conceived study, acquired funding, sampling design, CMH test
All authors edited the manuscript and approved the final version.

Data Availability

All analysis code is available on github (https://github.com/CoAdapTree and https://github.com/poojasingh09/2022_Singh_et_al_GWAS_SNC). All raw sequencing data will be deposited to the NCBI SRA (BioProject PRJNA867661).

References

Alexa A, Rahnenfuhrer J. **2019**. topGO: Enrichment Analysis for Gene Ontology.
Barton NH. **2000**. Genetic hitchhiking. *Philosophical transactions of the Royal Society of London. Series B, Biological sciences* **355**: 1553–1562.
Baucom RS, De Roode JC. **2011**. Ecological immunology and tolerance in plants and animals. *Functional Ecology* **25**: 18–28.
Bergot M, Cloppet E, Pérarnaud V, Déqué M, Marçais B, Desprez-Loustau M. **2004**. Simulation of potential range expansion of oak disease caused by Phytophthora cinnamomi under climate change. *Global Change Biology* **10**: 1539–1552.

Bernoux M, Timmers T, Jauneau A, Brière C, de Wit PJGM, Marco Y, Deslandes L. **2008**. RD19, an Arabidopsis cysteine protease required for RRS1-R-mediated resistance, is relocalized to the nucleus by the Ralstonia solanacearum PopP2 effector. *The Plant cell* **20**: 2252–2264.

Black BA, Shaw DC, Stone JK. **2010**. Impacts of Swiss needle cast on overstory Douglas-fir forests of the western Oregon Coast Range. *Forest Ecology and Management* **259**: 1673–1680.

Boyce JS. **1940**. A needle cast of Douglas Fir associated with Adelopus gaumanni. *Phyptopathology*. **30**: 649-655 pp.

Brandt RWilliam. **1960**. *The rhabdocline needle cast of Douglas fir*. Syracuse: State University College of Forestry.

Capitano BR. **1999**. The infection and colonization of Douglas-fir by P. gaeumannii.

Chastagner GA. **1990**. Maturation of apothecia and control of rhabdocline needlecast on Douglas-fir in western Washington. *Proceedings of conference on recent research on foliage diseases*: 87–92.

Chastagner GA. **2001**. Susceptibility of Intermountain Douglas-Fir to Rhabdocline Needle Cast When Grown in the Pacific Northwest. *Plant Health Progress* **2**: 2.

Cronn R, Dolan PC, Jogdeo S, Wegrzyn JL, Neale DB, St. Clair JB, Denver DR. **2017**. Transcription through the eye of a needle: daily and annual cyclic gene expression variation in Douglas-fir needles. *BMC Genomics* **18**: 558.

Evans N, Baierl A, Semenov MA, Gladders P, Fitt BDL. **2008**. Range and severity of a plant disease increased by global warming. *Journal of The Royal Society Interface* **5**: 525–531.

Falcone Ferreyra ML, Rius S, Casati P. **2012**. Flavonoids: biosynthesis, biological functions, and biotechnological applications . *Frontiers in Plant Science* **3**: 222.

Freeman B, Beattie G. **2008**. An Overview of Plant Defenses against Pathogens and Herbivores. *The Plant Health Instructor*.

Garrett KA, Dendy SP, Frank EE, Rouse MN, Travers SE. **2006**. Climate change effects on plant disease: genomes to ecosystems. *Annual review of phytopathology* **44**: 489–509.

Grabherr MG, Haas BJ, Yassour M, Levin JZ, Thompson DA, Amit I, Adiconis X, Fan L, Raychowdhury R, Zeng Q, *et al.* 2011. Full-length transcriptome assembly from RNA-Seq data without a reference genome. *Nature Biotechnology* **29**: 644–652.

Hammerschmidt R. **1999**. Induced disease resistance: how do induced plants stop pathogens? *Physiological and Molecular Plant Pathology* **55**: 77–84.

Hansen EM, Stone JK, Capitano BR, Rosso P, Sutton W, Winton L, Kanaskie A, McWilliams MG. **2000**. Incidence and Impact of Swiss Needle Cast in Forest Plantations of Douglas-fir in Coastal Oregon. *Plant Disease* **84**: 773–778.

Hart AJ, Ginzburg S, Xu M (Sam), Fisher CR, Rahmatpour N, Mitton JB, Paul R, Wegrzyn JL. **2020**. EnTAP: Bringing faster and smarter functional annotation to non-model eukaryotic transcriptomes. *Molecular Ecology Resources* **20**: 591–604.

Hill WG, Robertson A. **1968**. Linkage disequilibrium in finite populations. *Theoretical and Applied Genetics* **38**: 226–231.

Hill WG, Weir BS. **1988**. Variances and covariances of squared linkage disequilibria in finite populations. *Theoretical Population Biology* **33**: 54–78.

Howick VM, Lazzaro BP. **2017**. The genetic architecture of defence as resistance to and tolerance of bacterial infection in Drosophila melanogaster. *Molecular Ecology* **26**: 1533–1546.

Jirage D, Tootle TL, Reuber TL, Frost LN, Feys BJ, Parker JE, Ausubel FM, Glazebrook J. **1999**. Arabidopsis thaliana PAD4 encodes a lipase-like gene that is important for salicylic acid signaling. *Proceedings of the National Academy of Sciences* **96**: 13583 LP – 13588.

Johnson RF. **2002**. Genetic variation of Douglas-fir to Swiss needle cast as assessed by symptom expression. *Silvae Genetica* **51**: 80–8.

Juroszek P, Racca P, Link S, Farhumand J, Kleinhenz B. **2020**. Overview on the review articles published during the past 30 years relating to the potential climate change effects on plant pathogens and crop disease risks. *Plant Pathology* **69**: 179–193.

Kolomiets M V, Chen H, Gladon RJ, Braun EJ, Hannapel DJ. **2000**. A leaf lipoxygenase of potato induced specifically by pathogen infection. *Plant physiology* **124**: 1121–1130.

Kurkela T. **1981**. Growth reduction in Douglas fir caused by Rhabdocline needle cast [Pseudotsuga menziesii, height, radial increment, fungal diseases]. *Finnish Forest Research Institute*.

Lee EH, Beedlow PA, Waschmann RS, Tingey DT, Cline S, Bollman M, Wickham C, Carlile C. **2017**. Regional patterns of increasing Swiss needle cast impacts on Douglas-fir growth with warming temperatures. *Ecology and evolution* **7**: 11167–11196.

Lee M-H, Jeon HS, Kim SH, Chung JH, Roppolo D, Lee H-J, Cho HJ, Tobimatsu Y, Ralph J, Park OK. **2019**. Lignin-based barrier restricts pathogens to the infection site and confers resistance in plants. *The EMBO Journal* **38**: e101948.

Lefevere H, Bauters L, Gheysen G. **2020**. Salicylic Acid Biosynthesis in Plants . *Frontiers in Plant Science* **11**: 338.

Lind B. **2021a**. GitHub.com/CoAdapTree/varscan_pipeline.

Lind B. **2021b**. GitHub.com/brandonlind/cmh_test.

Lind BM, Lu M, Obreht Vidakovic D, Singh P, Booker TR, Aitken SN, Yeaman S. **2022**. Haploid, diploid, and pooled exome capture recapitulate features of biology and paralogy in two non-model tree species. *Molecular Ecology Resources* **22**: 225–238.

Lorenzo O, Piqueras R, Sánchez-Serrano JJ, Solano R. **2003**. ETHYLENE RESPONSE FACTOR1 integrates signals from ethylene and jasmonate pathways in plant defense. *The Plant cell* **15**: 165–178.

Ma Q-H, Xu Y. **2008**. Characterization of a caffeic acid 3-O-methyltransferase from wheat and its function in lignin biosynthesis. *Biochimie* **90**: 515–524.

Maguire D, Kanaskie A, Voelker W, Johnson R, Johnson G. **2002**. Growth of young Douglas-fir plantations across a gradient in Swiss needle cast severity. *Western Journal of Applied Forestry* **17**: 86–95.

Manter DK, Bond BJ, Kavanagh KL, Rosso PH, Filip GM. **2000**. Pseudothecia of Swiss needle cast fungus, *Phaeocryptopus gaeumannii*, physically block stomata of Douglas fir, reducing CO2 assimilation. *New Phytologist* **148**: 481–491.

Manter, Kelsey, Stone. **2001**. Quantification of *Phaeocryptopus gaeumannii* colonization in Douglas-fir needles by ergosterol analysis. *Forest Pathology* **31**: 229–240.

Manter DK, Winton LM, Filip GM, Stone JK. **2003**. Assessment of Swiss Needle Cast Disease: Temporal and Spatial Investigations of Fungal Colonization and Symptom Severity. *Journal of Phytopathology* **151**: 344–351.

Marroni F, Pinosio S, Zaina G, Fogolari F, Felice N, Cattonaro F, Morgante M. **2011**. Nucleotide diversity and linkage disequilibrium in Populus nigra cinnamyl alcohol dehydrogenase (CAD4) gene. *Tree Genetics and Genomes* **7**: 1011–1023.

Maynard Smith J, Haigh J. **1974**. The hitch-hiking effect of a favourable gene. *Genetics Research, Cambridge* **23**: 23–35.

Miller RNG, Costa Alves GS, Van Sluys M-A. **2017**. Plant immunity: unravelling the complexity of plant responses to biotic stresses. *Annals of botany* **119**: 681–687.

Mir AA, Park S-Y, Abu Sadat M, Kim S, Choi J, Jeon J, Lee Y-H. **2015**. Systematic characterization of the peroxidase gene family provides new insights into fungal pathogenicity in Magnaporthe oryzae. *Scientific reports* **5**: 11831.

Mishina TE, Zeier J. **2006**. The Arabidopsis flavin-dependent monooxygenase FMO1 is an essential component of biologically induced systemic acquired resistance. *Plant physiology* **141**: 1666–1675.

Mitchell-Olds T, Willis JH, Goldstein DB. **2007**. Which evolutionary processes influence natural genetic variation for phenotypic traits? *Nature Reviews Genetics* **8**: 845–856.

Montwé D, Elder B, Socha P, Wyatt J, Noshad D, Feau N, Hamelin R, Stoehr M, Ehlting J. **2021**. Swiss needle cast tolerance in British Columbia's coastal Douglas-fir breeding population. *Forestry: An International Journal of Forest Research* **94**: 193–203.

Neale DB, McGuire PE, Wheeler NC, Stevens KA, Crepeau MW, Cardeno C, Zimin A V, Puiu D, Pertea GM, Sezen UU, *et al.* 2017. The Douglas-fir genome sequence reveals specialization of the photosynthetic apparatus in Pinaceae. *G3: Genes|Genomes|Genetics* **7**: 3157 LP – 3167.

Nielsen R. **2005**. Molecular signatures of natural selection. *Annual Review of Genetics* **39**: 197–218.

Nurmberg PL, Knox KA, Yun B-W, Morris PC, Shafiei R, Hudson A, Loake GJ. **2007**. The developmental selector AS1 is an evolutionarily conserved regulator of the plant immune response. *Proceedings of the National Academy of Sciences of the United States of America* **104**: 18795–18800.

Pagán I, García-Arenal F. **2018**. Tolerance to Plant Pathogens: Theory and Experimental Evidence. *International Journal of Molecular Sciences* **19**.

Pandey S, Nelson DC, Assmann SM. **2009**. Two Novel GPCR-Type G Proteins Are Abscisic Acid Receptors in Arabidopsis. *Cell* **136**: 136–148.

Panikashvili D, Shi JX, Schreiber L, Aharoni A. **2009**. The Arabidopsis DCR encoding a soluble BAHD acyltransferase is required for cutin polyester formation and seed hydration properties. *Plant physiology* **151**: 1773–1789.

Parker AK. **1970**. Effect of Relative Humidity and Temperature on Needle Cast Disease of Douglas Fir. *Phytopathology* **60**: 1270.

Pusztahelyi T. **2018**. Chitin and chitin-related compounds in plant-fungal interactions. *Mycology* **9**: 189–201.

Remington DL, Thornsberry JM, Matsuoka Y, Wilson LM, Whitt SR, Doebley J, Kresovich S, Goodman MM, Buckler ES. **2001**. Structure of linkage disequilibrium and phenotypic associations in the maize genome. *Proceedings of the National Academy of Sciences* **98**: 11479 LP – 11484.

Restif O, Koella JC. **2004**. Concurrent evolution of resistance and tolerance to pathogens. *The American naturalist* **164**.

Ritóková G, Shaw DC, Filip G, Kanaskie A, Browning J, Norlander D. **2016**. Swiss Needle Cast in Western Oregon Douglas-Fir Plantations: 20-Year Monitoring Results. *Forests* **7**.

Rustérucci C, Montillet J-L, Agnel J-P, Battesti C, Alonso B, Knoll A, Bessoule J-J, Etienne P, Suty L, Blein J-P, *et al.* 1999. Involvement of Lipoxygenase-dependent Production of Fatty Acid Hydroperoxides in the Development of the Hypersensitive Cell Death induced by Cryptogein on Tobacco Leaves *. *Journal of Biological Chemistry* **274**: 36446–36455.

Serrano M, Coluccia F, Torres M, L'Haridon F, Métraux J-P. **2014**. The cuticle and plant defense to pathogens . *Frontiers in Plant Science* **5**: 274.

Sharma E, Anand G, Kapoor R. **2017**. Terpenoids in plant and arbuscular mycorrhiza-reinforced defence against herbivorous insects. *Annals of Botany* **119**: 791–801.

Shaw DC, Filip GM, Kanaskie A, Maguire DA, Littke WA. **2011**. Managing an epidemic of Swiss Needle Cast in the Douglas-Fir Region of Oregon: The role of the Swiss Needle Cast cooperative. *Journal of Forestry* **109**: 109–119.

Shaw DC, Ritóková G, Lan Y-H, Mainwaring DB, Russo A, Comeleo R, Navarro S, Norlander D, Smith B. **2021**. Persistence of the Swiss Needle Cast outbreak in Oregon coastal Douglas-Fir and new insights from research and monitoring. *Journal of Forestry*: 407–421.

Smith KF, Sax DF, Lafferty KD. **2006**. Evidence for the role of infectious sisease in species extinction and endangerment. *Conservation Biology* **20**: 1349–1357.

Stone J. **2018**. Swiss Needle Cast. In: Hansen EM, Lewis KJ, Chastagner GA, eds. Compendium of Conifer Diseases. St. Paul Minnesota, U.S.A.: APS Press, 111–114.

Stone JK, Capitano BR, Kerrigan JL. **2008a**. The histopathology of *Phaeocryptopus gaeumannii* on Douglas-fir needles. *Mycologia* **100**: 431–444.

Stone JK, Coop LB, Manter DK. **2008b**. Predicting effects of climate change on Swiss needle cast disease severity in Pacific Northwest forests. *Canadian Journal of Plant Pathology* **30**: 169–176.

Swiss Needle Cast Collective. **2011**. Swiss needle cast summary.

Temel F, Johnson GR, Adams WT. **2005**. Early genetic testing of coastal Douglas-fir for Swiss needle cast tolerance. *Canadian Journal of Forest Research* **35**: 521–529.

Temel F, Johnson GR, Stone JK. **2004**. The relationship between Swiss needle cast symptom severity and level of *Phaeocryptopus gaeumannii* colonization in coastal Douglas-fir (Pseudotsuga menziesii var. menziesii). *Forest Pathology* **34**: 383–394.

Tuladhar P, Sasidharan S, Saudagar P. **2021**. 17 - Role of phenols and polyphenols in plant defense response to biotic and abiotic stresses. In: Jogaiah SBT-BA and SM, ed. Woodhead Publishing, 419–441.

Wang J, Chai J. **2020**. Structural Insights into the Plant Immune Receptors PRRs and NLRs1. *Plant Physiology* **182**: 1566–1581.

Wang R-S, Pandey S, Li S, Gookin TE, Zhao Z, Albert R, Assmann SM. **2011**. Common and unique elements of the ABA-regulated transcriptome of Arabidopsis guard cells. *BMC genomics* **12**: 216.

Wegrzyn JL, Liechty JD, Stevens KA, Wu L-S, Loopstra CA, Vasquez-Gross HA, Dougherty WM, Lin BY, Zieve JJ, Martínez-García PJ, *et al.* 2014. Unique features of the loblolly pine (Pinus taeda L.) megagenome revealed through sequence annotation. *Genetics* **196**: 891–909.

Wilhelmi N, Bennett PI, Shaw DC, Stone JK. **2021**. *Rhabdocline Needle Cast of Douglas-fir*. Portland, Oregon, USA.

Wilhelmi NP, Shaw DC, Harrington CA, Clair JBS, Ganio LM. **2017**. Climate of seed source affects susceptibility of coastal Douglas-fir to foliage diseases. *Ecosphere* **8**.

Yang S, Li J, Zhang X, Zhang Q, Huang J, Chen J-Q, Hartl DL, Tian D. **2013**. Rapidly evolving R genes in diverse grass species confer resistance to rice blast disease. *PNAS* **110**: 18572 LP – 18577.

Young ND. **2003**. QTL MAPPING AND QUANTITATIVE DISEASE RESISTANCE IN PLANTS. *http://dx.doi.org/10.1146/annurev.phyto.34.1.479* **34**: 479–501.

Zhang X, Fend Z, Zhao L, Liu S, Wei F, Shi Y, Feng H, Zhu H. **2020**. Succinate dehydrogenase SDH1–1 positively regulates cotton resistance to Verticillium dahliae through a salicylic acid pathway. *Journal of Cotton Research* **3**: 12.

Zhang H, Gao Z, Zheng X, Zhang Z. **2012**. The role of G-proteins in plant immunity. *Plant signaling & behavior* **7**: 1284–1288.

Zhu C, Gore M, Buckler ES, Yu J. **2008**. Status and prospects of association mapping in plants. *The Plant Genome* **1**.

Zhu Z, Xu F, Zhang Y, Cheng YT, Wiermer M, Li X, Zhang Y. **2010**. Arabidopsis resistance protein SNC1 activates immune responses through association with a transcriptional corepressor. *Proceedings of the National Academy of Sciences of the United States of America* **107**: 13960–13965.

Supplementary Data

File S1 Sampling location information

File S2 Pooled sample information

File S3 Significant SNC and RNC SNPs and gene annotations and gene ontology annotations and enrichment.

Figure S1 Map of sampling locations for this study. See File S1 for more details.

Figure S2 PCA of SNP allele frequencies of (A) SNC and (B) RNC libraries.

Figure S3 Decay of Linkage disequilibrium (LD) calculated as r2 as a function of distance. r2 is the correlation of allele frequencies of SNC associated SNPs and 'neutral' SNPs on the same contig.

Figures

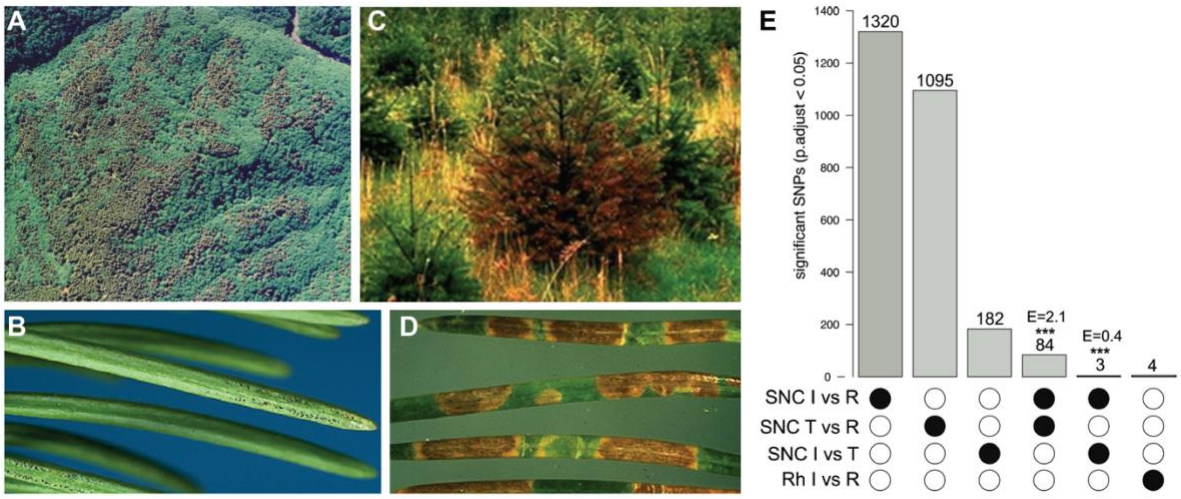

Figure 1 Damage in coastal Douglas-fir forests from (A) Swiss Needle Cast (SNC) disease caused by *Nothophaeocryptopus gaeumannii*. (B) *N. gaeumannii* infected Douglas-fir needles. (C) Rhabdocline Needle Cast (RNC) epidemic caused by *Rhabdocline pseudotsugae* in Pacific North-Western USA. (D) *R. pseudotsugae* infected Douglas-fir needles. (E) Number of significantly associated SNPs (FDR adjusted) from SNC and RNC GWAS analysis. Asterisks indicate greater than expected significant ($p < 0.005$) hypergeometric overlap across tests. Observed overlap indicated below the asterisk and expected overlap indicated above the asterisk. I = disease intolerant, R = disease resistant; T=disease tolerant.

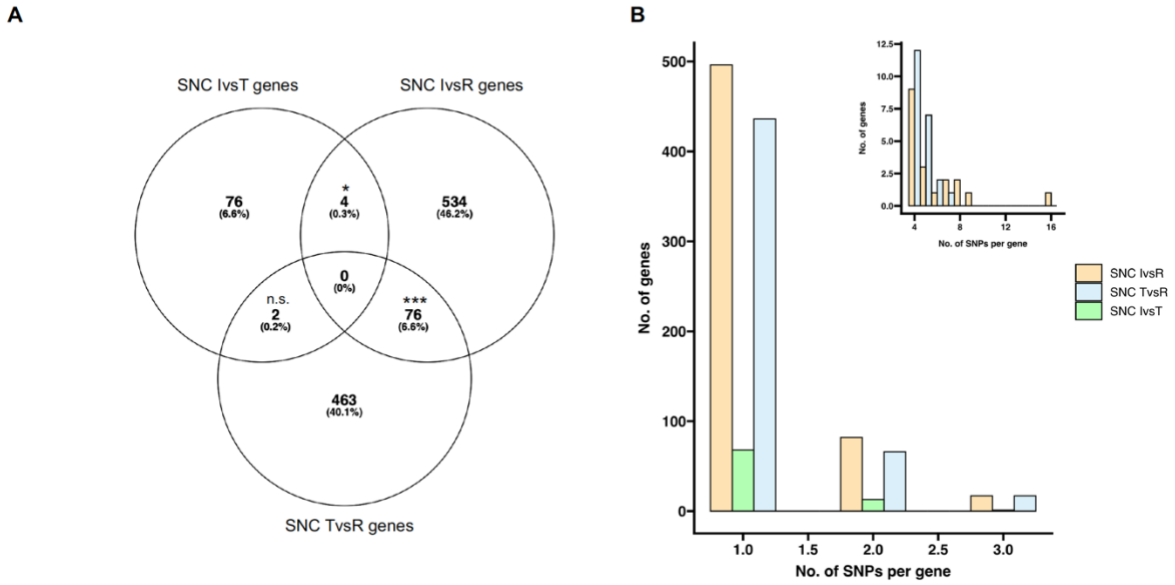

Figure 2 (A) Overlap of SNC tolerant and resistant candidate genes. Asterisks denote significant hypergeometric overlaps and n.s. denotes non-significant overlap (B) Number of significant SNPs per SNC candidate genes.

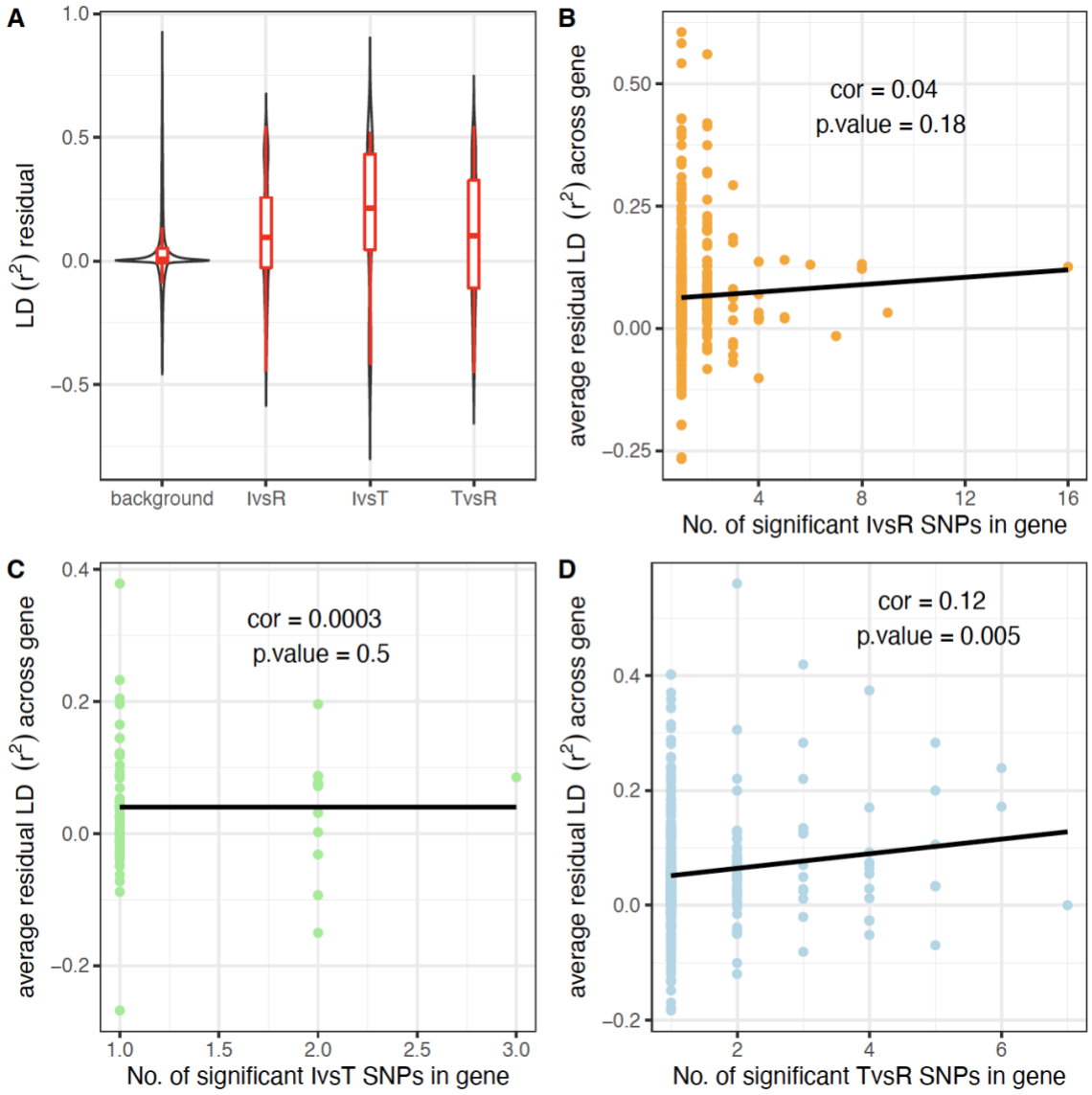

Figure 3 Overview of Linkage disequilibrium (LD) around SNC resistant and tolerant SNPs (A) Genome-wide LD residuals compared to LD residuals around SNC associated SNPs. LD is calculated as r^2 as a function of distance. For SNC associated SNPs, r^2 is the correlation of allele frequencies of significant SNC SNPs and 'neutral' SNPs on the same contig. Background LD is calculated using a random set of SNPs across the genome (see Methods). Residuals are the difference between the observed and expected LD (B, C, D) Relationship between the number of significant SNPs found per gene versus average LD across the gene.

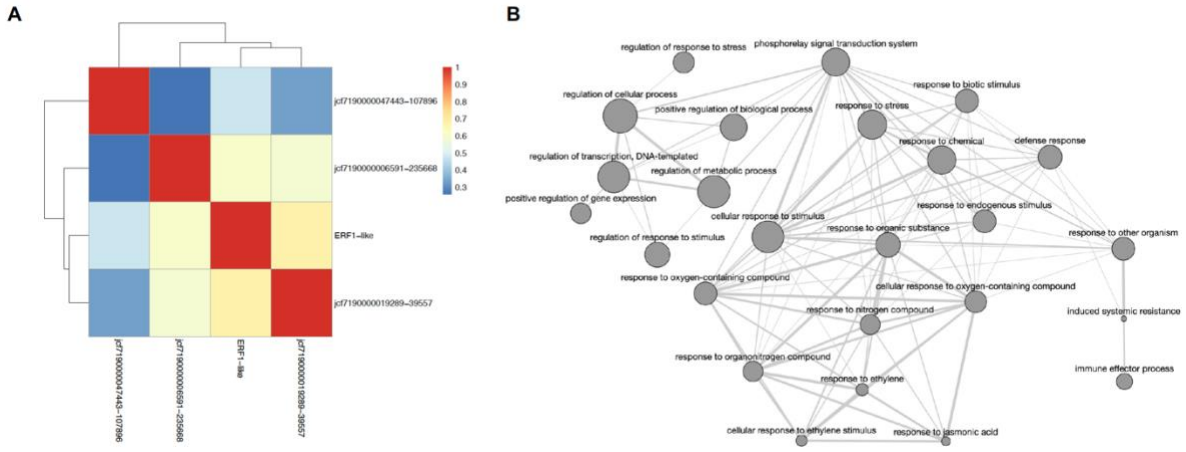

Figure 4 (A) Spearman's rho correlation of allele frequency of RNC significant SNPs. (B) Gene Ontology network of the biological processes associated with the ERF1 gene.